J. Chem. Soc., Faraday Trans. 1, 1989, **85**(7), 1723–1742

Infrared Spectroscopic Studies of the Reactions of Alcohols over Group IVB Metal Oxide Catalysts

Part 1.—Propan-2-ol over TiO_2, ZrO_2 and HfO_2

Gamal A. M. Hussein† and Norman Sheppard*
School of Chemical Sciences, University of East Anglia, Norwich NR4 7TJ
Mohamed I. Zaki and Radamis B. Fahim
Chemistry Department, Faculty of Science, Minia University, El Minia, Egypt

Infrared spectroscopy has been used to analyse the gas-phase reaction products and the related adsorbed species obtained between room temperature and 400 °C from the dehydrogenation/dehydration reactions of propan-2-ol over a series of differently calcined catalysts of TiO_2, ZrO_2 and HfO_2. The ZrO_2 and HfO_2 results were independent of the calcination pretreatment, and the surfaces of these oxides, like that from a TiO_2 sample calcined at 800 °C, were dehydroxylated. Different results were obtained from a TiO_2 sample calcined at 300 °C which had a hydroxylated surface. The acidic sites and reactivities of the surfaces of TiO_2(300 °C) and TiO_2(800 °C) were explored by pyridine adsorption and infrared spectroscopy. Only Lewis-acid sites were detected by pyridine.

On raising the reaction temperature, in all cases the dehydrogenation reaction to give acetone occurred either before or simultaneously to the onset of the dehydration reaction to give propene. Acetone production was most pronounced over ZrO_2 and HfO_2 but also occurred more with TiO_2(800 °C) than with TiO_2(300 °C). The dehydrogenation reaction was largely quenched by pre-adsorbed pyridine on both TiO_2 samples. The TiO_2 (300 °C) catalyst showed the presence of adsorbed propan-2-ol and 2-propoxide groups at room temperature. The dehydroxylated ZrO_2, HfO_2 and TiO_2(800 °C) samples only showed appreciable amounts of 2-propoxide groups. In each case the 2-propoxide ions occurred in two different forms, presumably formed by adsorption on different types of sites.

Both the acetone and propene products appeared as absorptions from 2-propoxide surface species decreased in intensity, so the latter are clearly reactive species. Gas-phase acetone production was followed by the chemisorption of acetone at a higher temperature. This subsequently decomposed to give surface acetate species, and finally at 400 °C to give CO_2 and methane in the gas phase. Propene did not give rise to adsorbed species, or to further products in the gas phase.

At the higher temperatures, above 300 °C, the reaction was always selective in favour of the dehydration reaction. However, each of the dehydroxylated catalysts showed some selectivity in favour of the dehydrogenation reaction over the earliest temperature range for alcohol decomposition, between 200 and 250 °C.

A discussion is given of possible mechanistic pathways for the production of surface 2-propoxide species and the two types of products, based on the infrared-supported assumption that the different adsorbed forms of 2-propoxide [and possibly adsorbed propan-2-ol on TiO_2(300 °C)] are reactive intermediates.

† On leave from Minia University.

The catalytic decomposition of alcohols, *via* dehydration and dehydrogenation reactions, is considered a straightforward means of producing materials of prime industrial importance.[1] Consequently, it has stimulated research curiosity, and a large number of papers have been published dealing with the subject from a range of important aspects;[2-7] the above-mentioned references provide examples. The catalysts tested have usually been based on metal oxides. The alcohols studied have been mostly those representing the world's largest feedstocks, *i.e.* ethanol and methanol, but mechanistic studies of isopropyl alcohol decompositions have also been fruitful. Experimental studies have made good use of chromatographic and mass-spectrometric techniques for gas-phase product analysis and lately, as in this paper, of vibrational spectroscopic methods for characterizing the surface species involved.[8-11]

However, problems inherent to the application of the infrared method to difficult catalyst materials (problems such as low specific surface area, difficulties in pressing coherent discs, or strong scattering or absorption of radiation by the catalyst) have so far caused difficulties in working with a number of good oxide catalysts of alcohol decomposition. Amongst these are Group IVB metal oxides, particularly ZrO_2 and HfO_2, which have until very recently[12,13] not been subjected to such investigations. We show that Fourier-transform infrared spectroscopy, with its intrinsic high sensitivity, can overcome many of these problems.

In an earlier study Zaki and Sheppard[10] found that propan-2-ol adsorbed on CeO_2 calcined at 400 °C gives rise to hydrogen-bonded alcohol and isopropoxide surface species at room temperature. At higher temperatures, up to 400 °C, first of all dehydrogenation gave rise to acetone in the gas phase (> 150 °C) and carboxylate surface species, and then (> 250 °C) propene was produced by the dehydration reaction. These findings are in general agreement with earlier conclusions on alumina.[8]

The present paper presents and discusses the results of a Fourier-transform infrared spectroscopic investigation of isopropyl alcohol decomposition between room temperature and 400 °C over TiO_2, ZrO_2 and HfO_2 catalysts which have themselves been calcined at different temperatures between 300 and 1000 °C. The principal goal was to correlate the results with surface textural and structural changes brought about by the different calcination treatments, in hopes of achieving a better understanding of the alcohol–surface reaction pathways. As described in more detail below, the effects of calcination were monitored by supplementary thermogravimetric (TG), differential thermal analysis (DTA), X-ray diffraction (XRD) and sorption isotherm measurements.

Experimental

Catalyst Materials: Pretreatment and Characterization Procedures

Titania (TiO_2-P25) was supplied by Degussa (W. Germany) with 99.5% purity. Zirconia (ZrO_2) and hafnia (HfO_2) were high-purity (99.9%) products from the Aldrich Chemical Co. Each of these oxides was thermally treated at 300, 500, 800 and 1000 °C, in each case for 5 h in a static atmosphere of air. For convenience the various calcination products are designated in the text by the chemical symbol for the oxide followed by the calcination temperature given in parentheses. Thus $TiO_2(300)$ indicates TiO_2 calcined for the standard 5 h at 300 °C.

The course of the calcination processes of the parent oxides was thermoanalytically explored by TG and DTA techniques which were applied, as has been described previously,[14] between room temperature and 1200 °C. The calcination products were further characterized by X-ray powder diffractometry and by infrared spectroscopy, also as described earlier.[14] Surface-area and porosity measurements of the samples were assessed by analysing N_2 sorption isotherms determined at −195 °C using, respectively, the B.E.T. and α_s methods.[15] Measurement of the isotherms was performed on a Carlo–Erba sorptomatic (Series 1800) instrument. The surface-acidity of some selected

TiO_2 samples was also probed by the adsorption of pyridine, followed by infrared spectroscopy (see below).

Infrared Spectroscopy

Infrared spectra were obtained at 4 cm^{-1} resolution between 4000 and 650 cm^{-1} using a Digilab FTS 20 V Fourier-transform spectrophotometer. The spectra were taken in a cell with an upper furnace section where the catalyst could be heated at various temperatures in the appropriate gas phase. After each heat treatment (see below) the catalyst disc in its holder was lowered into the infrared transmitting section of the cell, fitted with NaCl windows, for obtaining the spectrum of the (catalyst–adsorbed species–gas phase) at room temperature. By again raising the catalyst disc the spectrum of the gas phase could be measured separately. The spectrum of (catalyst–adsorbed species) was obtained by absorbance subtraction of, or transmission-ratioing with, the gas-phase spectrum. If necessary, the background spectrum of the initial catalyst in vacuum could also be subtracted or ratioed to give the spectrum of the adsorbed species alone.

A standard procedure was used for obtaining the spectra with the different catalysts. Self-supporting, but porous, thin wafers (*ca.* 20 mg cm^{-2}) of the catalyst were prepared from the powder in a hydraulic press. Satisfactory discs could be obtained from TiO_2 at a pressure of 2–4 ton† cm^{-2}; for ZrO_2 and HfO_2 10 ton cm^{-2} was necessary. After insertion into a holder the disc was pretreated in the infrared cell in a stream of O_2 (50 cm^3 min^{-1}) at 400 °C for 1 h, followed by evacuation at room temperature to *ca.* 5×10^{-5} Torr.‡

After recording the background spectrum of the (cell–catalyst) in vacuum, 10 Torr of the alcohol vapour (or 3 Torr of pyridine vapour) were admitted. The catalyst disc was then raised to the furnace section of the cell and heated consecutively in the resulting gaseous atmospheres at the specified temperatures for 10 min in each case. Spectra both of the gas phase and the adsorbed species were then obtained at room temperature as described above.

Reagents, Reference Compounds and Gases

Propan-2-ol and all other chemicals (acetone, pyridine, acetic acid and formic acid) were spectroscopic-grade BDH products. Prior to use they were thoroughly degassed by freeze–pump–thaw cycles performed under vacuum. Oxygen, nitrogen, propene, methane, CO_2 and CO were supplied by the British Oxygen Company in high purity (99.99%).

Results and Discussion

Physical Characterization of the Catalyst

TG and DTA analyses showed that originally uncalcined samples of TiO_2, ZrO_2 and HfO_2 all suffer a slight overall weight loss (< 2.7%) on heating to 1200 °C (at 20 °C min^{-1}) in four endothermic steps centred at *ca.* 120, 240, 400 and 600 °C. In addition, ZrO_2 gave rise to a fifth endothermic effect at *ca.* 1150 °C, although there was no corresponding weight change. The DTA curves of TiO_2 and HfO_2 showed notable baseline drifts commencing at 600 and 800 °C, respectively.

Since the three oxides showed rather uniform thermal behaviour below 600 °C, an infrared investigation of the chemical nature of the various processes involved was

† 1 ton = $1.016\,047 \times 10^3$ kg.

‡ 1 Torr ≈ 133.32 N m^{-2}.

Table 1. N_2-determined surface areas for TiO_2, ZrO_2 and HfO_2 calcined for 5 h at the temperatures indicated

	surface area/$m^2\ g^{-1}$			
catalyst	300 °C	500 °C	800 °C	1000 °C
TiO_2	69.4	77.3	14.3	9.5
ZrO_2	10.0	2.1	6.3	1.7
HfO_2	4.3	12.5	9.6	8.3

confined to the case of TiO_2. An infrared spectrum obtained from a self-supporting wafer of uncalcined TiO_2 indicated, after 10 min evacuation at room temperature, the existence of free OH groups [ν(OH) 3750–3640 cm^{-1}], and hydrogen-bonded OH groups [a broad (OH) adsorption between 3650 and 2800 cm^{-1}] from OH^- ions or adsorbed water molecules. The presence of a proportion of adsorbed water molecules was shown explicitly by a δ(HOH) absorption at 1620 cm^{-1}, and the presence of some carbonate surface species was indicated by absorptions in the 1570–1430 cm^{-1} range. At the weight-loss step at 120 °C, the infrared spectra showed the partial removal of water molecules and carbonate groups. After the next step of 240 °C these removals had been completed and the only ν(OH) absorptions remaining were at 3720, 3665 and 3640 cm^{-1} from OH groups free of hydrogen bonding. According to Tsyganenko and Filiminov,[16] these hydroxyl adsorptions denote terminal (3720 cm^{-1}) and two different types of bridged (3665 and 3640 cm^{-1}) surface OH groups. Recent low-temperature infrared spectra from CO on TiO_2 have disclosed that the bridged OH groups are relatively more acidic than the terminal ones.[17] The infrared spectra also suggest that the weight-loss at 400 °C involves further water elimination through condensation of pairs of OH groups;[18] after 600 °C the surface is almost completely dehydroxylated. It was also noted that thermoevacuation above 400 °C caused the wafer the change in colour from white to grey, with an associated loss in infrared transmission. Such a phenomenon has been encountered previously,[19] and was attributed to a release of lattice oxygen to give anionic vacancies and Ti^{3+} ions.

When matched with relevant ASTM standards for identification purposes, X-ray powder diffractograms confirmed that TiO_2(300) and (500) had the dominant monoclinic anatase structure, whereas TiO_2(800) and (1000) were of the tetragonal rutile structure. These results suggest that the baseline drift in the DTA curve above 600 °C can be attributed to the gradual anatase-to-rutile transformation. All the calcination products of ZrO_2 and HfO_2 showed XRD patterns (ASTM no. 3-340 for ZrO_2; no. 6-0318 for HfO_2) indicating the monoclinic structure. This is as expected, since the monoclinic to tetragonal transformation takes place at 1100 °C for ZrO_2 and 1600 °C for HfO_2. The 1150 °C endotherm shown by the DTA curve for ZrO_2 can clearly be attributed to this transformation, but the baseline drift above 800 °C for HfO_2 is most probably due to a sintering process rather than a phase transformation.

With respect to the textural consequences of calcination, N_2 adsorption studied at −195 °C gave, with all the catalysts, type II isotherms with type-H3 hystersis loops occurring at $P/P^\circ > 0.45$. A B.E.T. analysis of the isotherms gave the surface areas listed in table 1 and α_s analysis resulted in entirely linear plots passing through the origin. The textural significance of these results is that the catalysts and their calcination products have inaccessible particle porosity. The H-3 hysteresis loops most likely are due to adsorbate condensation occurring in interparticle voids of slit-shaped form.

Table 2. Frequencies/cm^{-1} of infrared bands of pyridine adsorbed at ambient temperature on the surface of TiO_2(500) and (800), compared to reference data from the literature indicated

this work			ref. (18)		ref. (20)
liquid pyridine	Ti(500)	Ti(800)	TiO_2 (anatase)	TiO_2 (rutile)	TiO_2 (anatase)
1439 vs	1440 vs	1440 vs	1445 vs	1445 vs	1440 vs
1482 s	1490 s	1490 s	1484 s	1484 s	1488 s
1572 s, sh	1575 s	1575 m	1572 m	1572 m	1572 m
1580 vs	1605 vs	1610 vs	1605 vs	1605 vs	1602 vs
—	1637 vw	—	1635 w	—	1637 w

vs = very strong, s = strong, m = medium, w = weak, sh = shoulder.

The TiO_2 Catalyst Surface Acidity as Probed by Pyridine Adsorption and Infrared Spectroscopy

Infrared spectra from pyridine adsorbed at ambient temperature on TiO_2(500) (mainly of anatase structure with a hydroxylated surface) and on TiO_2(800) (a pure rutile with a nearly completely dehydroxylated surface) displayed the bands listed in table 2, where they are compared with relevant literature values. Bands at 1537 or 1440 cm^{-1} are considered[20] to indicate the existence of pyridinium ions bonded to Brønsted-acid sites (protonic OH) or pyridine coordinated to Lewis-acid sites (coordinatively unsaturated titanium ions), respectively. The results recorded in table 2 imply[18, 20] that the surfaces of TiO_2(500) and TiO_2(800) only expose Lewis-acid sites. The additional, very weak band observed for TiO_2(500) at 1637 cm^{-1} is probably due to physisorbed water, since a companion weak and broad ν(OH) band occurs very near 3200 cm^{-1}. A 10 min thermoevacuation at 150 °C, followed by cooling *in vacuo* to ambient temperature, resulted in the reduction of this band with the simultaneous reappearance of bands due to free surface OH groups.

For both TiO_2(500) and TiO_2(800), evacuation at 400 °C led to a substantial reduction in intensity of the pyridine bands listed in table 2, and the growth of a new band at *ca.* 1470 cm^{-1}. This new band was particularly strong in the case of TiO_2(800) and is probably associated with pyridine adsorption on sites of particularly high Lewis acidity.[21]

Infrared Analysis of the Gas Phases resulting from Propan-2-ol Decomposition over the Oxide Catalysts

TiO_2

Fig. 1 shows the gas-phase spectra following the introduction of a 10 Torr dose of propan-2-ol over TiO_2(300), followed by successive 10 min contacts with this catalyst at the temperatures indicated. After each heating, the cell is cooled down to room temperature before the infrared spectrum is taken. Propan-2-ol remains the spectroscopically dominant gas-phase species at room temperature or after heating to 150 °C [spectrum (*a*)]. At 200 °C the products propene and acetone, with diagnostic bands at 910 and 1740 cm^{-1}, respectively [spectrum (*b*)]. After heating at 250 °C [spectrum (*c*)] the propan-2-ol was completely converted to products, with propene dominant together with a small amount of acetone (band at 1740 cm^{-1}). Propene was the spectroscopically dominant product at all temperatures investigated. At 300 °C the amount of acetone was

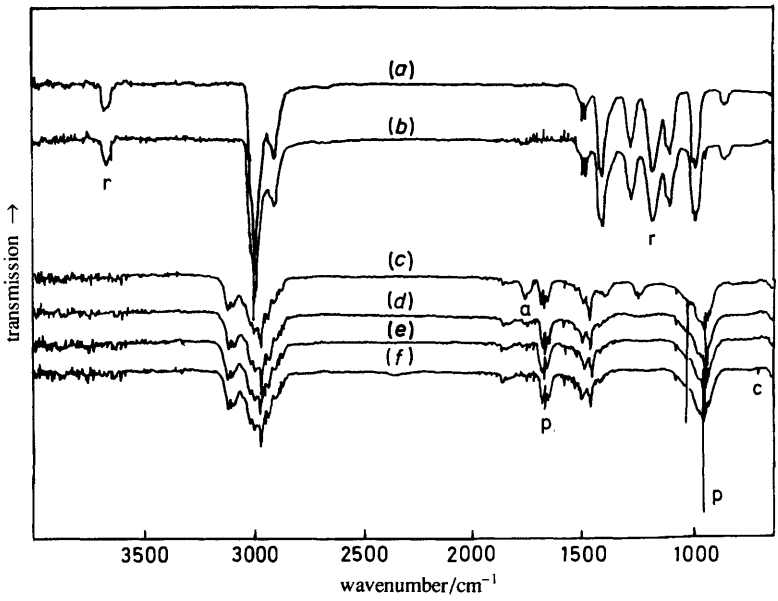

Fig. 1. Room-temperature infrared spectra from 10 Torr propan-2-ol after being in contact with TiO_2(300) for 10 min at (*a*) room temperature and 150 °C; (*b*) 200; (*c*) 250; (*d*) 300, (*e*) 350 and (*f*) 400 °C. Principal infrared absorption bands used for the estimation of the amounts of the reactant propan-2-ol (r) and the products acetone (a); propene (p); and CO_2 (c) are indicated.

much reduced and it had completely disappeared at 350 °C. At 400 °C very weak bands from a new product CO_2 (2350 and 667 cm^{-1}) could be observed.

Similar spectra were recorded to determine the gas-phase products from 10 Torr propan-2-ol over TiO_2(500) and TiO_2(800). It was not possible to press coherent wafers from TiO_2(1000). The results for TiO_2(500) did not differ much from those for TiO_2 (300), but significant differences occurred with TiO_2(800). These are that (i) acetone was the first product, appearing at 200 °C; (ii) propan-2-ol was still present in the gas-phase at 250 °C, at which temperature propene started to appear; (iii) at 300 °C the alcohol was completely decomposed, the amount of acetone had increased but propene had become the dominant product; (iv) at 350 °C the amount of acetone had decreased again; and (v) at 400 °C, some acetone still remained, but bands from a small amount of methane as well as CO_2 had appeared.

By using infrared intensity calibration curves derived from measurements of the individual pure gas-phase species as a function of pressure, in the same infrared cell and under the same spectroscopic conditions, it is possible to derive quantitative analyses of the gas mixtures from the infrared data, as summarised in fig. 2 for TiO_2(300) and TiO_2(800). The values for TiO_2(500) are similar to those for TiO_2(300). The reduced activity of the TiO_2(800) catalyst for propene formation, and its increased activity for acetone formation compared with TiO_2(300), are clearly shown in fig. 2. The TiO_2(800) catalyst has a high selectivity (but still limited reactivity) for acetone formation between 200 and 250 °C. At the higher temperatures both catalysts were highly selective for propene formation. The fact that the sum of the pressures of propene and acetone are less than the 10 Torr pressure of the original alcohol can be accounted for partly by the presence of the other gas-phase products methane and CO_2, and partly by the retention of adsorbed residues on the catalyst itself, as will be discussed later.

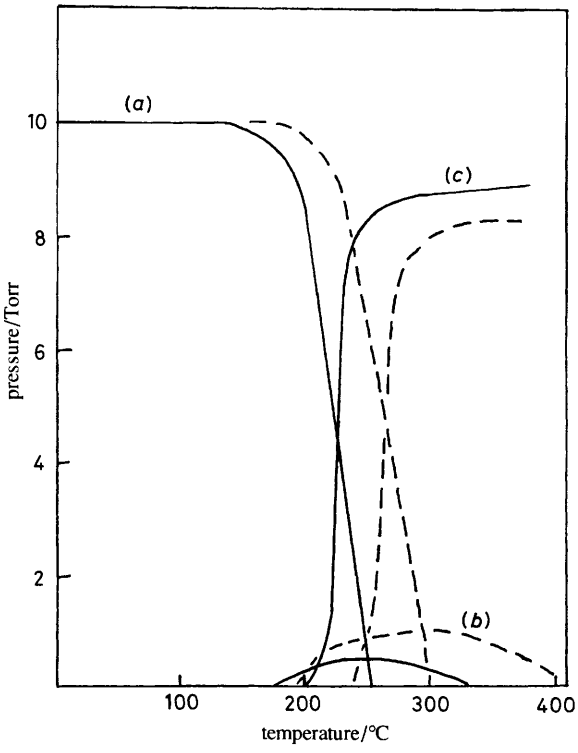

Fig. 2. Infrared quantitative analysis of the gas-phase composition showing the relation between the reaction temperature and the pressure (Torr), resulting from an initial dose of 10 Torr of the reactant propan-2-ol (*a*) giving rise to the products acetone (*b*) and propene (*c*) after consecutive 10 min intervals at the temperatures indicated over the catalysts TiO_2(300) (——) and TiO_2(800) (- - - - -).

ZrO_2 *and* HfO_2

The corresponding analytical results, derived from infrared spectra, for ZrO_2(500) and HfO_2(500) are shown in fig. 3. Virtually identical results were obtained for the other calcination products from each of these oxides. Even the two different oxides are seen to give rather similar results. The pattern of results resembles that obtained from TiO_2(800) rather than from TiO_2 (300) but goes even further in the direction of acetone formation. Below about 300 °C the reaction over ZrO_2 is selective for acetone. Above 300 °C the selectivity moves in favour of propene for both oxides although not to the same degree as with the TiO_2 catalysts. Once again, as the concentration of gas-phase acetone decreased, at the high temperature of 400 °C small amounts of methane and CO_2 were produced.

TiO_2 *Precovered with Pyridine*

Following Miyata *et al.*,[20] who studied the vanadia–titania system, it was considered that it would be of interest to see how the decomposition pathways might be modified by blocking some of the Lewis-acid sites with pyridine. This was performed by taking gas-phase alcohol and product spectra in the usual way over TiO_2(500) and TiO_2(800) discs which had been pretreated with 3 Torr pyridine at 400 °C as described earlier. The

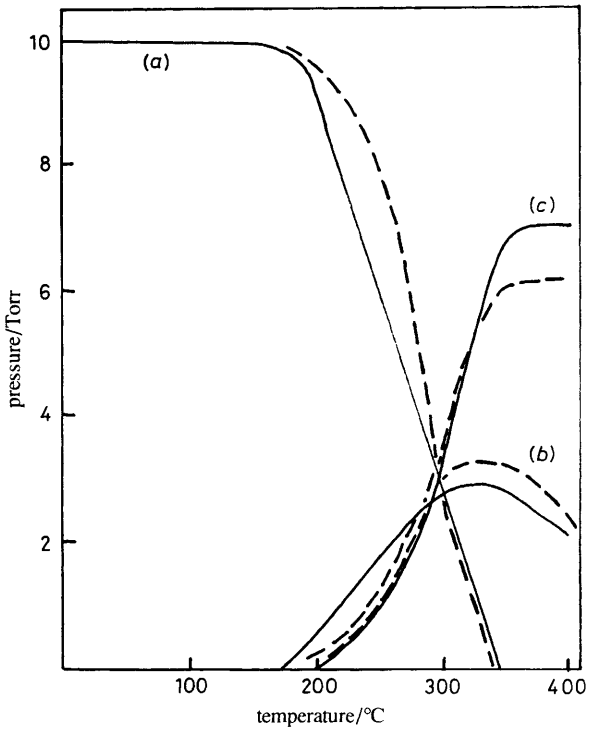

Fig. 3. As for fig. 2, except that the catalysts are ZrO_2(500) (——) and HfO_2(500) (- - - - -).

derived analytical results for the TiO_2(500) sample are shown in fig. 4 in comparison with those obtained over the clean TiO_2 sample, repeated from fig. 2.

Pyridine pre-adsorption on the TiO_2(500) sample suppressed acetone formation, presumably by blocking the sites which are active in the dehydrogenation reaction, and also slowed down the dehydration reaction to form propene. On TiO_2(800) the main effect was the suppression of acetone formation, *i.e.* in both cases pyridine pre-adsorption markedly increased the selectivity of the TiO_2 catalysts in favour of the dehydration reaction.

Infrared Analyses of the Adsorbed Species Resulting from Propan-2-ol Decomposition over the Oxide Catalysts

Spectra were obtained of the adsorbed species at each step in the reaction procedures already discussed that gave rise to the gas-phase spectra. After each temperature treatment, the spectra were obtained after cooling to room temperature in the presence of the gase phase. The gas contributions were ratioed-out to give the spectra illustrated below. In a few cases the initial spectrum of the clean catalyst was also ratioed-out.

TiO_2(300) *and* TiO_2(800)

The spectra on this oxide were the best defined because of the good infrared transmission properties of the pressed discs. Spectra of adsorbed species were recorded for TiO_2(300), (500) and (800). However, as the (300) and (500) results were very similar, only those from TiO_2(300) and TiO_2(800) are illustrated in fig. 5 and 7. Fig. 6 illustrates selected spectra

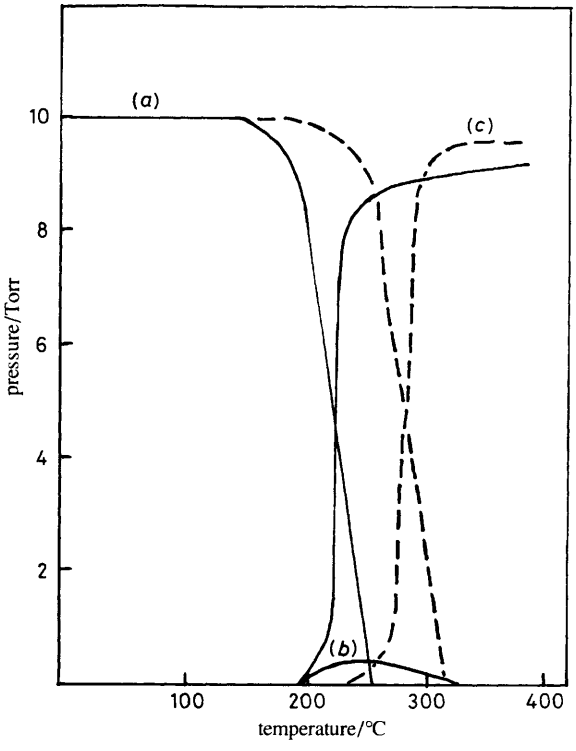

Fig. 4. As for fig. 2, except that the catalysts are $TiO_2(500)$ (——) and $TiO_2(500)$ with pre-adsorbed pyridine (- - - - -). See the text.

between 1800 and 800 cm^{-1} additionally ratioed against the background spectrum of the oxide.

In fig. 5 from $TiO_2(300)$, spectrum (*a*) illustrates that of the clean disc, and shows the three sharp absorptions at 3720, 3665 and 3640 cm^{-1} from the surface OH groups mentioned earlier. In spectrum (*b*) these bands have been removed, doubtless in part through their hydrogen-bonding interactions with physically adsorbed propan-2-ol so that they now contribute to the broad hydrogen-bonded ν(OH) adsorption between 3500 and 3000 cm^{-1}. This broad region has a sharper superimposed absorption at *ca.* 3445 cm^{-1} which has recently been assigned to ν(OH) of an undissociated but coordinated alcohol molecule.[22] The absorptions in the ν(CH) region and below 1500 cm^{-1} are listed in table 3 and are as expected for adsorbed propan-2-ol or the derived 2-propoxide.[20, 22, 23] The broad absorption at 1630 cm^{-1} is from adsorbed water, resulting initially from reaction of the alcohol with OH groups on the TiO_2 surface (see below) and later from the dehydration reaction. This surface water also undoubtedly contributes to the broad ν(OH) hydrogen-bonding absorption.

Fig. 6(*a*) and 6(*b*) illustrate more closely the 1800–800 cm^{-1} region of the room temperature from $TiO_2(300)$ and $TiO_2(800)$ after interaction with propan-2-ol at room temperature. The extra absorption on $TiO_2(300)$ at 1280 cm^{-1} is from the δ(OH) mode showing the presence of the physically adsorbed alcohol as well as the alkoxide ion.[22] This absorption is missing from the spectrum on $TiO_2(800)$ [fig. 6(*b*)] where most of the alcohol has probably been converted to the 2-propoxide ion. The remaining bands are very close to those observed in the spectra of a range of $M(2\text{-propoxide})_4$ compounds including M = Ti, Zr and Hf (table 3).[24]

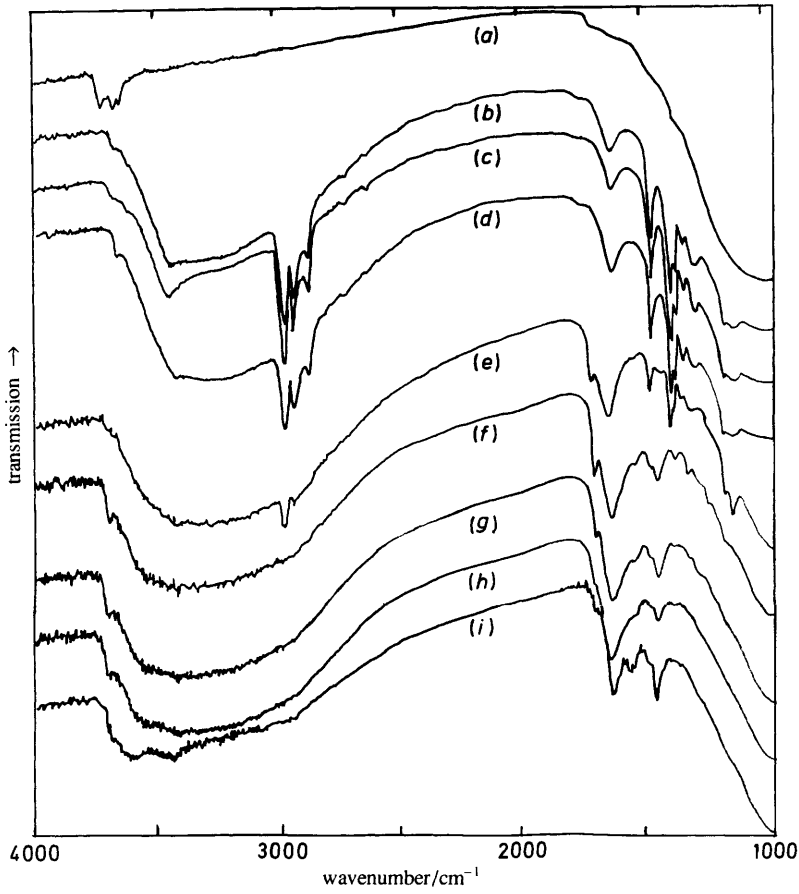

Fig. 5. Room-temperature infrared spectra from species adsorbed on TiO_2(300) after 10 Torr of propan-2-ol had been consecutively held for 10 min in the presence of the catalyst at (*b*) room temperature; (*c*) room temperature after evacuation (separate experiment); (*d*) 200, (*e*) 250, (*f*) 300, (*g*) 350, (*h*) 400 and (*i*) 400 °C, after evacuation. (*a*) Background spectrum of the TiO_2(300) catalyst before the introduction of propan-2-ol.

Over TiO_2(300) the alcohol–alkoxide absorptions drastically diminish at 250 °C, which is the temperature at which the absorption bands from adsorbed water substantially strengthen. At this temperature, propan-2-ol has also been replaced in the gas phase largely by the dehydration product propene and to a lesser extent by the dehydrogenation product acetone. In the spectrum of the adsorbed species a shoulder also develops at 1700 cm^{-1} from adsorbed acetone as was confirmed by a spectrum from the adsorption of acetone on a clean TiO_2 disc. At 300 °C and above, new absorption bands from adsorbed species occurred at 1540–1550 (s), 1470 (w), 1440 (s) and 1385 (w) cm^{-1} due to surface acetate ions, an assignment which was confirmed by a spectrum from the adsorption of acetic acid on a clean TiO_2 disc. Evacuation at 400 °C led to weakening of the ν(OH) and $\delta(H_2O)$ bands, so as to show the acetate bands more clearly. It also leads to regrowth of absorption due to hydrogen-bond free surface OH groups. The assignments of the bands from the adsorbed species and from reference spectra are listed in table 4.

Analogous spectra of adsorbed species on TiO_2(800) are shown in fig. 7 and 6(*b*) and the bands are listed in tables 3 and 4. The background TiO_2 spectrum [fig. 7(*a*)] shows that this is a mostly dehydroxylated sample. The same surface species are present as

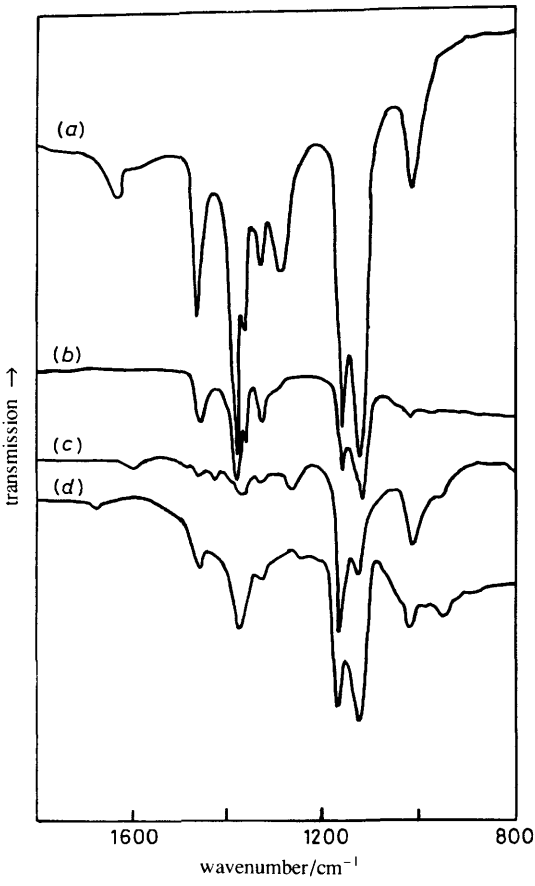

Fig. 6. Infrared spectra of the surface species from the adsorption of 10 Torr propan-2-ol at room temperature on the catalysts (*a*) $TiO_2(300)$; (*b*) $TiO_2(800)$; (*c*) $ZrO_2(500)$ and (*d*) $HfO_2(500)$.

before but between 300 and 400 °C the bands from adsorbed acetone and from the associated acetate species are more prominent. In this case the water band at 1630 cm^{-1} does not appear until 300 °C, at which temperature propene dominates in the gas phase (fig. 2) together with some acetone. From 150 °C upwards a sharp absorption occurs near 3420 cm^{-1} which will be the subject of later discussion. The differential type feature near 2960 cm^{-1} arises from miscancellation of the strong band from propan-2-ol in the gas phase.

It is worth noting that for $TiO_2(800)$, whereas substantial acetone is easily detected in the gas phase by 250 °C, the band from adsorbed acetone does not appear until 300 °C; it seems that the adsorption process is activated. From the spectra in fig. 7 from $TiO_2(800)$ it is particularly clear that the acetate bands appear at the same temperature as those from adsorbed acetone. Both acetone and acetate absorptions weaken somewhat at 400 °C at which temperature small amounts of CO_2 and methane appear in the gas phase.

$ZrO_2(500)$ *and* $HfO_2(500)$

The overall transmission of the pressed discs from ZrO_2 and HfO_2 was very poor, partly because of heavy scattering of higher frequencies by these relatively low-area oxides, and possibly also partly because of a broad continuous electronic absorption above

Table 3. Observed frequencies/cm^{-1} of principal absorptions from surface species produced by adsorption of propan-2-ol on TiO_2, ZrO_2 and HfO_2 catalysts at room temperature (fig. 6), compared with those from model compounds

assignments	TiO_2(300)	TiO_2(800)	ZrO_2(500)	HfO_2(500)	Ti[O(2-Pr)]$_4$[a]	Zr[O(2-Pr)]$_4$[a]	Hf[O(2-Pr)]$_4$[a]
ν(OH)	3500–3000 s, vb[b,c]	3500–3000 w, v bd	*ca.* 3550 w, bd	*ca.* 3500 w, bd	—	—	—
$\nu(CH_3)$ as	2975 vs	2970 s	2970 s	2970 s	2959	2950 vs	2941
$2\times\delta(CH_3)$ as	2935 s	2935 ms	2930 w	2930 ms	2924	2899 s	2882
$\nu(CH_3)$	2870 ms	2870 m	2865 w	2865 vw	2857	2849 s	
$\delta(H_2O)$[c]	1630 m[c]	—	—	—			
$\delta(CH_3)$ as	1465 m	1465 ms	1465 w	1465 m	1462, 1451	1465 s	1475
$\delta(CH_3)$ s	1385 s	1385 s	1380 m	1380 s	1391, 1381	1379 s	1379
	1365 m, sh	1365 m, sh		—	1370	1360 s	1364
δ(CH)	1340 w	1349 m	1340 w	1340 w	1328	1333 m	1348
δ(OH)[d]	1280 m	—	1260 m	—	1248	—	
ν(CO)	1170 vs	1170 s	1170 vs	1170 vs	1159	1166 vs	1186, 1170
ν(CC)		1138 ms, sh					
CH_3 rock	1130 vs	1130 s	1130 s	1130 vs	1124	1136 vs	1140
	1030 m	1030 w	1030 ms	1030 m	1000	1007 vs	1020
					950	958 s	983

[a] Ref. (24). vs = very strong, s = strong, m = medium, w = weak, vw = very weak, sh = shoulder, bd = broad, vb = very broad; 2-Pr = 2-propoxide; [b] breadth caused by hydrogen-bonding; [c] adsorbed water; [d] δ(OH) from undissociated propan-2-ol.

Table 4. Observed frequencies/cm^{-1} of principal absorption bands produced from surface species by reaction of propan-2-ol at 400 °C over TiO_2, ZrO_2 and HfO_2 catalysts, compared with those from acetone and acetic acid adsorbed separately on TiO_2(800). All spectra were measured at room temperature

TiO_2(300)	TiO_2(800)	ZrO_2(300)	HfO_2(300)	acetone on TiO_2(800)	acetic acid on TiO_2(800)	assignments
1700 w, sh	1700 m	1690 w	1700 m	1693 vs		ν(C=O) (acetone)
1620 vs	1630 m	1590 m, sh	1600 m, sh	(1600 mw)		$\delta(H_2O)$
1550 m	1550 m	1555 s	1550 m		1550 s	$\nu(CO_2)^-$ (a) acetate
	ca. 1530 m					
1475 w						
1440 s	1440 vs	1435 s	1440 s	1445 w	1440 vs	$\nu(CO_2)^-$ (s) acetate

vs = very strong, s = strong, m = medium, w = weak, vw = very weak, sh = shoulder.

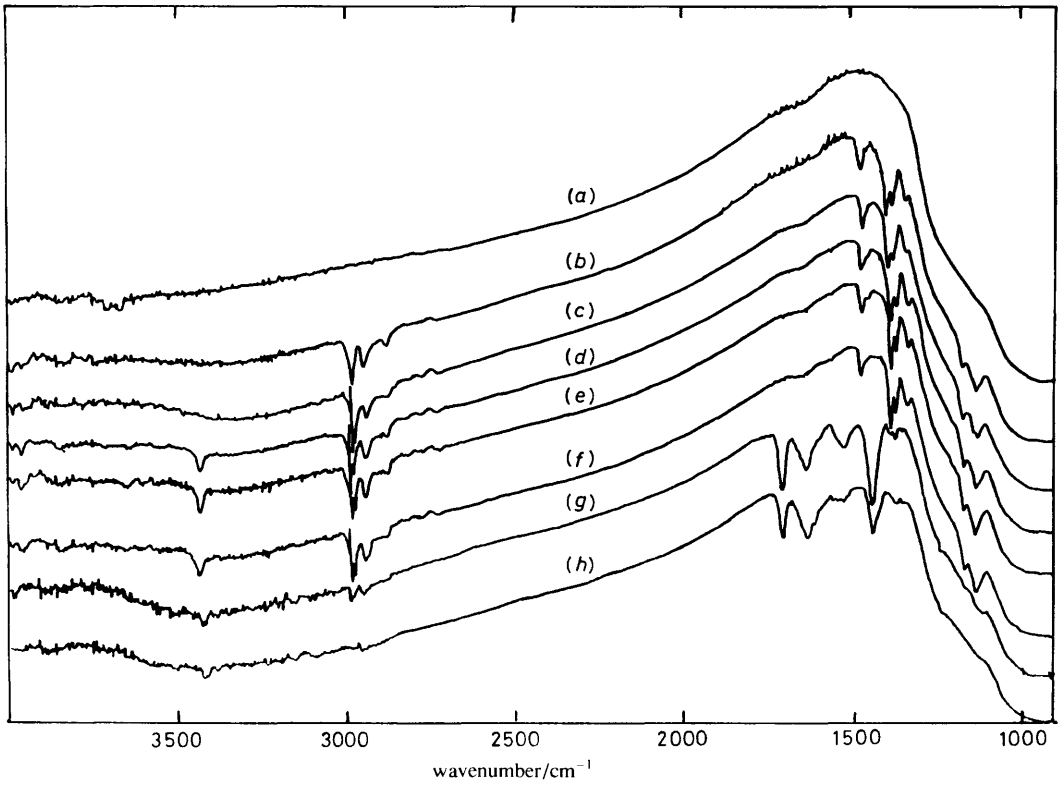

Fig. 7. Room-temperature infrared spectra from species adsorbed on TiO_2(800) after 10 Torr of propan-2-ol had been adsorbed and then (*b*) evacuated at room temperature; (*c*) in the presence of 10 Torr propan-2-ol followed consecutively by heating for 10 min at room temperature; (*d*) 150, (*e*) 200, (*f*) 250, (*g*) 300 and (*h*) 400 °C. (*a*) is the background spectrum of the TiO_2(800) catalyst before the introduction of the propan-2-ol.

1400 cm^{-1} such as can be associated with semiconductivity properties.[25] The two oxides exhibited lattice-mode blackout absorptions below *ca.* 800 cm^{-1} and gave steeply sloping background spectra from 800 to *ca.* 1800 cm^{-1}. Above the latter frequency only the strong (CH) bands from adsorbed 2-propoxide or propan-2-ol could be discerned.

Spectra from pressed discs of ZrO_2(500) and Hf(500) were studied in more detail. The frequencies and intensities of the absorption bands measured after propan-2-ol addition, both at room temperature and after heating in 50 °C stages up to 400 °C, are listed in tables 3 and 4, in comparison with the corresponding data for the TiO_2 catalysts. The room temperature spectra are also compared with those from TiO_2(300) and TiO_2(800) in fig 6(*c*) and (*d*).

It is seen in fig. 6 and table 3 that at room temperature there are substantial differences in the relative intensities of bands in the 1200–1100 cm^{-1} ν(C–O)/ν(C–C) region, at *ca.* 1170 and 1130 cm^{-1} within the 2-propoxide dominated spectra from TiO_2(800), ZrO_2(500) and HfO_2(500). Such pairs of absorptions have previously been observed from methanol and ethanol on TiO_2 and assigned by Shchekochikhin *et al.*[26] to the presence of two different alkoxide surface species. More specifically Tsyganenko *et al.*[16] and Lavalley *et al.*[13] have assigned the higher frequency to an alkoxide coordinated to a single metal cation, and the lower frequency one to an alkoxide bridge-bonded to two metal cations. In the propan-2-ol case there are complications because the pure alkoxides[24] have a pair of absorptions at *ca.* 1170 and 1130 cm^{-1}. However, the notable differences in the relative intensities of these pairs of bands, shown in fig. 6 for the different oxides, suggests that in this case also two alkoxide species are present, as has been demonstrated more clearly for adsorbed [$^2H_6$]propan-2-ol by Ross *et al.*[22]

Overall it can be concluded that the adsorption behaviours and the catalytic selectivities of ZrO_2 and HfO_2 are closely similar and that, although more favourable to acetone production, they are not dissimilar to those of TiO_2(800). All three catalysts have highly dehydroxylated surfaces and have a high exposure of Lewis-acid sites.

TiO_2 *after Adsorption of Pyridine at* 400 °C

In common with the conclusions from the gas-phase products (see above) the spectra of the surface species on TiO_2(500) and TiO_2(800) after pyridine pre-adsorption showed at 300 °C a notable weakening of absorptions from adsorbed 2-propoxide species, the generation of water (1630 cm^{-1}) from the dehydration reaction, but only weak absorptions from adsorbed acetone or surface acetate. The spectra of the surface species were very similar to those observed on the original clean, *i.e.* untreated, catalysts, but for TiO_2(500) showed a slower decomposition of 2-propoxide. The TiO_2(800) spectrum with pre-adsorbed pyridine shows particularly clearly at 400 °C a pair of sharp absorptions at *ca.* 3650 and 3400 cm^{-1} which have been previously attributed[27] to the rehydration of a rutile surface to give two different surface OH^- ions according to the equation

$$O^{2-}(s) + H_2O \rightleftharpoons 2OH^-(s) \qquad (1)$$

where (s) denotes a surface species. The same features are probably present in the spectra from adsorbed species at 400 °C for all the TiO_2 samples, but are more difficult to discern because of band-overlap.

Mechanistic Considerations in the Light of the Infrared Results

The Nature of the Oxide Surfaces

In this paper we shall formulate all the surface reactions using the convention that the oxides are ionic in structure. From the evidence cited above, TiO_2(300), ZrO_2 and HfO_2 all possess the monoclinic, anatase-type, structure whereas TiO_2(800) has the orthorhombic rutile structure. However, the last three samples have in common that their surfaces are strongly dehydroxylated and hence can only present Lewis-acid sites.

$TiO_2(300)$ on the other hand has absorptions from three types of surface OH^- as cited above, of which the high-frequency one has been assigned to OH^- coordination to a single Ti^{4+} ion, and the lower-frequency ones to bridged coordination to two Ti^{4+} ions.[16] Although it has been shown that these different types of surface OH^- have different acidities,[17] it is seen from the results of the pyridine-adsorption experiments that even $TiO_2(300)$ shows no Brønsted activity, *i.e.* proton transfer, to pyridine; the less-basic alcohol is even less likely to be a proton acceptor.

Primet *et al.*,[18] through the use of pyridine adsorption, had earlier concluded that there are two types of Lewis-acid sites on anatase and on rutile. We observe similar pyridine absorptions to those recorded by Primet, but also a fairly prominent band at *ca.* 1470 cm^{-1} at the higher temperature of 400 °C, probably from an additional Lewis-acid site (table 2).

2-Propoxide and Adsorbed Propan-2-ol as Surface Species

Since the pioneering infrared studies of Babushkin and Uvarov,[28] and of Greenler,[29] it has been generally accepted[8, 11, 26–34] that the alcohols over oxide surfaces lead to a mixture of adsorbed alcohol molecules and alkoxide species.

Adsorbed alcohol molecules could be held through hydrogen bonding to the surface as in eqn (2) and (3) below, or through coordination to a Ti^{4+} ion as in eqn (4).

$$OH^-(s) + ROH \rightarrow O\text{—}H^- \cdots O\text{—}R(s) \quad (2)$$

$$O^{2-}(s) + ROH \rightarrow O\text{—}H \cdots O^{2-}(s) \quad (3)$$

$$L^{n+}(s) + ROH \rightarrow L^{n+}(s) \cdots O\text{—}R(s) \quad (4)$$

where R denotes an alkyl group, and L^{n+} a Lewis-acid cationic metal site.

2-Propoxide formation could occur in two straightforward ways as in (5) and (6)

$$ROH + L^{n+}(s) + OH^-(s) \rightarrow RO^- \cdots L^{n+}(s) + H_2O\uparrow \quad (5)$$

$$ROH + L^{n+}(s) + O^{2-}(s) \rightarrow RO^- \cdots L^{n+}(s) + OH^-(s). \quad (6)$$

Clearly reactions (2) and (5) can only occur on a hydroxylated surface such as $TiO_2(300)$, whereas reactions (3), (4) and (6) can occur on dehydroxylated surfaces such as $TiO_2(800)$, ZrO_2 (500) or HfO_2 (500).

The narrower $\nu(OH)$ absorption near 3445 cm^{-1} in fig. 5(*b*) and 5(*c*) shows the presence of coordinated alcohol molecules from reaction (4).[22] That reaction (5) also occurs on $TiO_2(300)$ at room temperature is clearly shown by the absorption band from adsorbed water at 1630 cm^{-1} in fig. 5; the adsorbed water also undoubtedly contributes to the broad hydrogen-bonded OH absorption between 3500 and 3000 cm^{-1}. Reaction (5) also contributes to the removal of the sharp $\nu(OH^-)$ absorptions between 3750 and 3600 cm^{-1}. However, it is very probable that the spectral change is also brought about by the hydrogen bonding of OH^- ions to alcohol molecules, as in reaction (2). This would displace remaining sharp $\nu(OH^-)$ absorptions so that they also contribute to the broad 3500–3000 cm^{-1} band. Independent evidence that adsorbed alcohol as well as alkoxide species occur on $TiO_2(300)$ is provided by the spectrum of fig. 6(*a*). As mentioned earlier, compared with fig. 6(*b*) and 6(*d*) obtained on dehydroxylated surfaces, there is an additional absorption at *ca.* 1280 cm^{-1} which can be assigned to the $\delta(OH)$ (in-plane) mode of the adsorbed alcohol molecules (table 3). In fig. 6(*a*) the

ν(C—O)/ν(C—C) absorptions at 1170 and 1130 cm^{-1} probably include contributions for the adsorbed alcohol as well as alkoxide species.

The dehydroxylated surface of TiO_2(800) only shows ν(C—O)/ν(C—C) bands from two 2-propoxide surface species [fig. 6(*b*)] and not from adsorbed alcohol. As water molecules are not observed until 300 °C, when the dehydration reaction has taken place, the 2-propoxide groups are probably produced by reaction (6). This reaction requires the generation of new OH^-(s) groups and these are probably represented by a very broad and weak absorption band between *ca.* 3500 and 3000 cm^{-1} in the room-temperature spectrum, fig. 7(*b*). By 150 °C a sharp ν(OH) absorption at *ca.* 3420 cm^{-1} replaces the previous broad and weak one. The *ca.* 3420 cm^{-1} band is well known in the spectra of hydroxylated rutile[35, 27, 11] and has been attributed to highly coordinated OH^- groups which occur just below the surface, but which nevertheless retain surface reactivity as in H to D exchange with D_2O.[35] The increase from room temperature to 150 °C has probably provided the energy of activation necessary for the proton from an originally formed surface OH^- to move to the more stable subsurface location.

The Dehydrogenation Reaction

From the point of view adopted here, in which the oxides are discussed in essentially ionic terms, the dissociation of a neutral molecule into two neutral products is likely to involve heterolytic processes involving pairs of acid and base sites, whereas a covalent oxide formulation could lead to homolytic reaction steps; reality is probably somewhere between these two extremes.

Formally then, the removal of two hydrogen atoms from propan-2-ol to give H_2 and acetone is at some stage likely to involve a basic site to accept H^+ from the OH group, and an acidic site to accept H^- from the tertiary carbon atom, the two sites preferably existing close together. The formation of the product H_2 might alternatively occur in a concerted manner involving both H^+/H^- transfers subsequent to the formation, in this context, of pairs of OH^- and Ti^{3+}—H species. For example on ZnO, hydrogen itself reversibly dissociates to give Zn^+—H and OH^- ions on a particular type of $Zn^{2+}O^{2-}$ acid/base pair.[36]

Considering first the dehydroxylated TiO_2(800) surface, the spectroscopic evidence suggests that the 2-propoxide species are reactive intermediates, because these disappear from the surface as the dehydrogenation reaction commences, *i.e.* that the first step in the reaction is that described in eqn (6). There is indeed generally agreement that the acetone is derived from an alkoxide surface species.[8, 11, 31]

The second step could be, specifically to the propan-2-ol case

$$(CH_3)_2CHO^- \cdots Ti^{4+}(s) \rightarrow (CH_3)_2C{=}O\uparrow + H{-}Ti^{3+}(s) \qquad (7)$$

followed by

$$OH^-(s) + HTi^{3+}(s) \rightarrow H_2\uparrow + O^{2-}(s) + Ti^{4+}(s). \qquad (8)$$

Deo[8] has proposed, as an alternative to (7) and (8), a concerted reaction involving two hydrogen atoms as in eqn (9)

$$(CH_3)_2CHO^- \cdots Ti^{4+}(s) + OH^-(s) \rightarrow (CH_3)_2C{=}O\uparrow + H_2\uparrow + O^{2-}(s) + Ti^{4+}(s) \qquad (9)$$

with the surface OH^- providing the nucleophilic attack on the C_α carbon. As no further intermediates have been detected spectroscopically between the 2-propoxide and the final products, the present results cannot distinguish between these two alternative possibilities.

The fact that acetone production is notably stronger over TiO_2(800) than over TiO_2(300), and that it is quenched by pyridine preadsorption, shows clearly that its reaction mechanism occurs on Lewis-acid sites in the absence of OH^- groups on the original surface, *i.e.* that the alternative reaction (5), which could also lead to 2-propoxide ions, is unlikely to be involved in dehydrogenation.

We have referred above to the infrared evidence for the presence of two distinguishable 2-propoxide ions on TiO_2(800), ZrO_2 or HfO_2 and it would be of interest to determine which of them correlates with dehydrogenation or dehydration. Both of the relevant absorptions near 1170 and 1130 cm^{-1} weaken markedly when the two reactions commence (fig. 5 and 7) but, unfortunately, it is difficut to discern from the present spectra which weakens first. The situation is not helped by the relatively small temperature interval between the onset of the two different reactions, and this point deserves further spectroscopic investigation.

The Formation of Surface Acetate and Subsequently CO_2 *and Methane in the Gas phase*

These reactions are discussed at this point because there is general agreement that these later products are derived from adsorbed alkoxide,[8,9,11,29,34] and very probably from adsorbed acetone as the intermediates.[8,11,32] It is noteworthy (from comparisons of fig. 1, 5; 2 and 7) that adsorbed acetone on TiO_2(800) occurs at a rather higher temperature than that necessary for the production of acetone in the gas phase, *i.e.* that its adsorption is an activated process.

Deo *et al.*[8] have proposed that the production of surface acetate from adsorbed acetone occurs according to eqn (10)

$$(CH_3)_2CO\cdots Ti^{4+}(s) + OH^-(s) \rightarrow CH_3CO_2^-\cdots Ti^{4+}(s) + CH_4\uparrow \qquad (10)$$

and that CO_2 is later produced by decomposition of the surface acetate. A possibility for the latter reaction could be as in eqn (11)

$$CH_3CO_2^-\cdots Ti^{4+}(s) + OH^-(s) \rightarrow CO_2\uparrow + CH_4\uparrow + Ti^{4+}(s) + O^{2-}(s). \qquad (11)$$

On this scheme the overall catalysed reaction is seen to be

$$(CH_3)_2CO + H_2O \rightarrow 2CH_4 + CO_2. \qquad (12)$$

with the water from the parallel dehydration reaction supplying the two intermediate OH^- groups by reaction (1).

Fig. 5 and 7 show that acetate is indeed only produced in the presence of chemisorbed acetone. Also at the highest temperature of 400 °C the acetate absorptions disappear or weaken with in most cases the simultaneous observation of weak absorptions from CO_2 and methane in the gas phase. However, possibly because the gas-phase methane absorptions are at best weak, there is as yet no firm spectroscopic evidence that methane is produced simultaneously with the generation of surface acetate and before the production of CO_2 as required by eqn. (10).

The Dehydration Reaction

This reaction occurs on both hydroxylated and dehydroxylated surfaces. There have been differences of opinion in the literature as to whether, over alumina, the reaction intermediate is an adsorbed alcohol[8,31] or alkoxide,[11,33] but Tamaru *et al.*[33] have produced some infrared kinetic evidence in favour of the alkoxide intermediate. Miyaka *et al.*[11] have more recently supported this mechanism over TiO_2.

From the ionic point of view we will again consider the overall reaction formally to involve heterolytic processes involving acid–base pairs of sites.[37] Ultimately the acidic T^{4+}(s) site could accept an OH^- ion, and the basic O^{2-}(s) site a proton to give another OH^-(s). Product water would then be produced from the two OH^-(s) species as in the reverse reaction of eqn (1); alternatively, the water may be produced in a concerted reaction.

The long-standing Ipatieff mechanism[38] assumes the alkoxide species to be the

intermediate and envisages the overall reaction on a hydroxylated surface to involve reaction (5) above, followed in this context by

$$(CH_3)_2CHO^- \cdots Ti^{4+}(s) \rightarrow CH_3CH{=}CH_2\uparrow + OH^-(s) \cdots Ti^{4+}(s). \qquad (13)$$

On a dehydroxylated surface such as $TiO_2(800)$, $ZrO_2(500)$ or HfO_2 (500), reaction (6) would be the alternative first step, and (13) would then be followed by the condensation of the two $OH^-(s)$ to give the water product.

Alternative proposed mechanisms for the dehydration reaction involve (i) carbonium-ion formation as suggested by Whitmore,[39] either by proton-donation from the surface to the alcohol, or from direct decomposition to $(CH_3)_2CH^+$ and OH^- on a dehydroxylated surface (such mechanisms do account for isomerisation or alkene products with some larger alcohols[37]), or (ii) concerted reactions such as

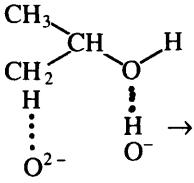

$$\rightarrow CH_3CH{=}CH_2\uparrow + H_2O\uparrow + OH^-(s) + O^{2-}(s) \qquad (14)$$

as suggested by Euken *et al.*,[40,41] Deo *et al.*[8] or in an alternative form suggested by Knözinger *et al.*[5]

None of these alternative mechanisms involved alkoxide ions directly, but rather adsorbed alcohol or carbonium ions, and therefore the infrared evidence does not favour them for the dehydroxylated surfaces. Also on $TiO_2(800)$ the Lewis-acid site responsible for dehydration above 250 °C must be different from that for dehydrogenation as the former reaction is not quenched by pyridine pre-adsorption.

However, $TiO_2(300)$ and $TiO_2(500)$ do have substantial additional dehydration activity at lower temperatures ($\leqslant$ 250 °C) compared with $TiO_2(800)$, as shown in fig. 2 and 4. As we have shown that the $TiO_2(300)$ or $TiO_2(500)$ surfaces also have adsorbed alcohol, the enhanced activity may be related to a contribution from the alternative mechanism. The fact that this additional reactivity is eliminated by pyridine pre-adsorption on $TiO_2(500)$ (fig. 4) could be taken as evidence that it is associated with a different type of Lewis-acid site on the originally hydroxylated surface. However, the reduced activity might alternatively be associated with infrared evidence that pyridine pre-adsorption removes a substantial proportion of the original surface OH^- ions.

Conclusions

Infrared analysis of the gas phase showed that all the TiO_2, ZrO_2 and HfO_2 catalysts studied show a selectivity preference for the dehydration reaction of propan-2-ol between 300 and 400 °C. However, a limited selectivity towards dehydrogenation occurred at intermediate temperatures above 200 °C except in the case of the hydroxylated $TiO_2(300)$ sample. In general, a higher proportion of acetone was generated over the dehydroxylated catalysts $TiO_2(800)$, $ZrO_2(500)$ and $HfO_2(500)$, with the latter two being most effective in this respect. At lower temperatures, $TiO_2(300)$ showed adsorbed alcohol and alkoxide, but only the latter, probably in two forms, occurred appreciably on the other three catalysts. The surface alkoxides were removed in the temperature range whether either dehydrogenation or dehydration was occurring and they therefore seem to be reactive intermediates.

The combined gas phase and surface infrared results are consistent with reactions (6) and (9) being responsible for the dehydrogenation reaction, followed by the decomposition of chemisorbed acetone to surface carboxylate and then gas-phase CO_2 and methane, perhaps according to reactions (10) and (11). The spectroscopic results

also showed that (presumably different) surface alkoxides are involved in the dehydration reaction according, on the dehydroxylated surfaces, to the modified Ipatieff mechanism involving (6) and (13). On the hydroxylated TiO_2(300) an Ipatieff mechanism involving reaction (5) instead of (6), or other mechanisms involving adsorbed alcohol as an intermediate, may also contribute to the catalytic process.

We are grateful to Professor K. S. W. Sing of Brunel University for allowing us to make the N_2 sorption measurements in his laboratory, and to Mr D. H. Chenery for assistance with practical spectroscopic techniques. One of us (G.A.M.H.) thanks the Egyptian Government for maintenance and travel grants.

References

1 I. Wender, *Catal. Rev.*, 1984, **26**, 304.
2 E. F. McCaffrey, D. G. Klissurski and R. A. Ross, *Catal. Vol. 1, Proc. 5th ICC*, Miami Beach, Florida, ed. J. W. Hightower (North-Holland/American Elsevier, 1972), pp. 151–159.
3 J. Cunningham, B. K. Hodnett, M. Ilyas, J. Tobin and E. L. Leahy, *Faraday Discuss. Chem. Soc.*, 1981, **72**, 283.
4 O. V. Krylov, *Catalysis by Non-Metals* (Academic Press, New York, 1970), pp. 115.
5 H. Knözinger, H. Buhl and K. Kochloefl, *J. Catal.*, 1972, **24**, 57; H. Knözinger and W. Stuhlin, *Prog. Colloid Polym. Sci.*, 1980, **67**, 33.
6 L. Nondek and J. Sedlacek, *J. Catal.*, 1975, **40**, 34; L. Nondek and M. Kraus, *J. Catal.*, 1975, **40**, 40.
7 R. B. Fahim, M. I. Zaki and R. M. Gabr, *Appl. Catal.*, 1982, **4**, 189.
8 A. V. Deo, T. T. Chuang and I. G. Dalla-Lana, *J. Phys. Chem.*, 1971, **75**, 234.
9 W. Hertl and M. A. Cuenca, *J. Phys. Chem.*, 1973, **77**, 1120.
10 M. I. Zaki and N. Sheppard, *J. Catal.*, 1983, **80**, 114.
11 T. Nakajima, H. Miyata and Y. Kubokawa, *Bull. Chem. Soc. Jpn*, 1982, **55**, 609.
12 M. Y. He and J. G. Ekerdt, *J. Catal.*, 1984, **87**, 381.
13 M. Bensitel, V. Moravek, J. Lamotte, O. Sauer and J. C. Lavalley, *Spectrochim. Acta, Part A*, 1987, **43**, 1487.
14 M. I. Zaki, H. M. Ismail and R. B. Fahim, *Surf. Interface Anal.*, 1986, **8**, 185.
15 K. S. W. Sing, *Surface Area Determination*, ed. D. H. Everett and R. H. Ottewill (Butterworths, London, 1970), p. 25.
16 A. A. Tsyganenko and V. N. Filiminov, *J. Mol. Struct.*, 1973, **19**, 579.
17 M. I. Zaki and H. Knözinger, *Mater. Chem. Phys.*, 1987, **17**, 201.
18 M. Primet, P. Pichat and M. V. Mathieu, *J. Phys. Chem.*, 1971, **75**, 1221.
19 G. D. Parfitt, *Progress in Surface and Membrane Science*, ed. N. F. Daniell (Academic Press, London, 1987), vol. 11, p. 186.
20 H. Miyata, Y. Nakagama, T. Ono and Y. Kubakawa, *J. Chem. Soc., Faraday Trans. 1*, 1983, **79**, 2343.
21 E. P. Parry, *J. Catal.*, 1963, **2**, 371.
22 P. F. Ross, G. Busca, V. Lorenzelli, O. Saur and J. C. Lavalley, *Langmuir*, 1987, **3**, 52.
23 V. N. Filimonov, *Kinet. Katal. (Russ.)*, 1966, **7**, 512.
24 C. T. Lynch, K. S. Mazdiyasni, J. S. Smilli and W. J. Crawford, *Anal. Chem.* 1964, **36**, 2332.
25 F. Boccuzzi, C. Morterra, R. Scala and A. Zecchina, *J. Chem. Soc., Faraday Trans. 2*, 1981, **77**, 2059.
26 V. M. Shchekochikhin, V. N. Filiminov, N. P. Keier and A. N. Terenin, *Kinet. Katal. (Russ.)*, 1964, **5**, 113.
27 J. Graham, C. H. Rochester and R. Rudham, *J. Chem. Soc., Faraday Trans. 1*, 1981, **77**, 1973 and 2735.
28 A. A. Babushkin and A. V. Uvarov, *Dokl. Akad. Nauk. USSR*, 1956, **110**, 581.
29 R. G. Greenler, *J. Chem. Phys.*, 1962, **37**, 2094.
30 R. O. Kagel, *J. Phys. Chem.*, 1967, **71**, 844.
31 Y. Yakerson, L. Lafer and A. Rubenstein, *Dokl. Acad. Nauk USSR*, 1967, **174**, 111.
32 A. V. Kiselev and U. V. Uvarov, *Surf. Sci.*, 1967, **6**, 399.
33 Y. Soma, T. Onishi and K. Tamaru, *Trans. Faraday Soc.*, 1969, **65**, 2215.
34 J. Graham, R. Rudham and C. H. Rochester, *J. Chem. Soc., Faraday Trans. 1*, 1984, **80**, 894.
35 P. Jones and J. A. Hockey, *Trans. Faraday Soc.*, 1971, **67**, 2669, 2679.
36 R. P. Eischens, W. A. Pliskin and M. J. D. Low, *J. Catal.*, 1962, **1**, 180.
37 H. Pines and J. Manassen, *Adv. Catal.*, 1966, **16**, 49.
38 V. N. Ipatieff, *Catalysis Reactions at High Pressures and Temperatures* (Macmillan, New York, 1936), pp. 60–120.
39 F. C. Whitmore, *J. Am. Chem. Soc.*, 1932, **54**, 3274.
40 A. Euken, *Naturwissenschaften*, 1944, **32**, 161.
41 A. Euken and E. Wicke, *Z. Naturforsch.*, 1947, **2**, 163.

Paper 8/02916D; *Received* 19*th July*, 1988